Experimental Lung Research

ISSN: 0190-2148 (Print) 1521-0499 (Online) Journal homepage: http://www.tandfonline.com/loi/ielu20

Mediation of the single-walled carbon nanotubes induced pulmonary fibrogenic response by osteopontin and TGF-β1

Timur O. Khaliullin, Elena R. Kisin, Ashley R. Murray, Naveena Yanamala, Michael R. Shurin, Dmitriy W. Gutkin, Liliya M. Fatkhutdinova, Valerian E. Kagan & Anna A. Shvedova

To cite this article: Timur O. Khaliullin, Elena R. Kisin, Ashley R. Murray, Naveena Yanamala, Michael R. Shurin, Dmitriy W. Gutkin, Liliya M. Fatkhutdinova, Valerian E. Kagan & Anna A. Shvedova (2017) Mediation of the single-walled carbon nanotubes induced pulmonary fibrogenic response by osteopontin and TGF-β1, Experimental Lung Research, 43:8, 311-326, DOI: 10.1080/01902148.2017.1377783

To link to this article: https://doi.org/10.1080/01902148.2017.1377783

Published online: 15 Nov 2017.

EXPERIMENTAL LUNG RESEARCH
2017, VOL. 43, NO. 8, 311–326
https://doi.org/10.1080/01902148.2017.1377783

Taylor & Francis
Taylor & Francis Group

ORIGINAL ARTICLE

Mediation of the single-walled carbon nanotubes induced pulmonary fibrogenic response by osteopontin and TGF-β1

Timur O. Khaliullin[a,b], Elena R. Kisin[b], Ashley R. Murray[b], Naveena Yanamala[b], Michael R. Shurin[c], Dmitriy W. Gutkin[c], Liliya M. Fatkhutdinova[d], Valerian E. Kagan[e], and Anna A. Shvedova[a,b]

[a]Department of Physiology & Pharmacology, West Virginia University, Morgantown, WV; [b]Exposure Assessment Branch, NIOSH/CDC, Morgantown, WV; [c]Department Pathology, University of Pittsburgh, Pittsburgh, PA; [d]Department of Hygiene and Occupational Medicine, Kazan State Medical University, Kazan, Russia; [e]Department of Pathology, University of Pittsburgh, Pittsburgh, PA

ABSTRACT

Purpose of the study: A number of *in vivo* studies have shown that pulmonary exposure to carbon nanotubes (CNTs) may lead to an acute local inflammatory response, pulmonary fibrosis, and granulomatous lesions. Among the factors that play direct roles in initiation and progression of fibrotic processes are epithelial-mesenchymal transition and myofibroblasts recruitment/differentiation, both mediated by transforming growth factor-β1 (TGF-β1). Yet, other contributors to TGF-β1 associated signaling, such as osteopontin (OPN) has not been fully investigated. **Materials and Methods:** OPN-knockout female mice (OPN-KO) along with their wild-type (WT) counterparts were exposed to single-walled carbon nanotubes (SWCNT) (40 μg/mouse) via pharyngeal aspiration and fibrotic response was assessed 1, 7, and 28 days post-exposure. Simultaneously, RAW 264.7 and MLE-15 cells were treated with SWCNT (24 hours, 6 μg/cm^2 to 48 μg/cm^2) or bleomycin (0.1 μg/ml) in the presence of OPN-blocking antibody or isotype control, and TGF-β1 was measured in supernatants. **Results and Conclusions:** Diminished lactate dehydrogenase activity at all time points, along with less pronounced neutrophil influx 24 h post-exposure, were measured in broncho-alveolar lavage (BAL) of OPN-KO mice compared to WT. Pro-inflammatory cytokine release (IL-6, TNF-α, MCP-1) was reduced. A significant two-fold increase of TGF-β1 was found in BAL of WT mice at 7 days, while TGF-β1 levels in OPN-KO animals remained unaltered. Histological examination revealed marked decrease in granuloma formation and less collagen deposition in the lungs of OPN-KO mice compared to WT. RAW 264.7 but not MLE-15 cells exposed to SWCNT and bleomycin had significantly less TGF-β1 released in the presence of OPN-blocking antibody. We believe that OPN is important in initiating the cellular mechanisms that produce an overall pathological response to SWCNT and it may act upstream of TGF-β1. Further investigation to understand the mechanistic details of such interactions is critical to predict outcomes of pulmonary exposure to CNT.

ARTICLE HISTORY
Received 11 April 2017
Accepted 6 September 2017

KEYWORDS
Carbon nanotubes; Lung fibrosis; Osteopontin; Pulmonary exposure; TGF-β1

Introduction

The carbonaceous nanomaterials family includes nanosized carbon black, fullerenes and graphene including its allotropic modifications – carbon nanotubes (CNT), which come in single- and multi-walled varieties. Single-walled carbon nanotubes (SWCNT) are among the most prospective of nanoparticles and are currently of great interest for many applications in electronics, composite materials, building construction, enhanced electron/scanning microscopy imaging techniques, biosensors and biomedicine.[1] They are also steadily making their way into general consumer products.[2] The global market for nanocomposites, including CNTs, has been reported to reach $5.3 billion by 2021 from $1.6 billion in 2016 at a compound annual growth rate of 26.7%.[3]

By now multiple studies have shown that SWCNTs in occupationally relevant doses cause pulmonary fibrosis with a rapid inflammatory onset and subsequent granulomas formation, thickening of the alveolar wall, and collagen deposition in rodents.[4–16] CNTs in general have been proposed as a model of chronic granulomatous lung inflammation.[17] SWCNT might be even more damaging as their clearance from the lungs seems to take longer than their multi-walled CNT (MWCNT) counterparts and their alveolar retention period may span 100 days or more after initial exposure.[17,18] Alveolar macrophages might have

CONTACT Dr. Anna A. Shvedova ats1@cdc.gov CDC/NIOSH/HELD, Exposure Assessment Branch, 1095 Willowdale Road, Morgantown, WV 26505, USA.
Color versions of one or more of the figures in the article can be found online at www.tandfonline.com/ielu.

difficulties recognizing SWCNT as a foreign material, leading to the improved fibers' penetration and accumulation in the lung interstitium.[9,16,19,20] In human lung fibroblasts, SWCNT caused significantly increased expression of transforming growth factor beta 1 (TGF-β1) and TGF-β Receptor 1, as well as collagen production compared to MWCNT-exposed cells.[21] Importantly, parallels have been drawn between SWCNT-induced pathology and interstitial pulmonary fibrosis (IPF) or other similar conditions involving formation of fibroblast/myofibroblast foci.[22]

Previous research has provided evidence for the role of TGF-β1 and another known factor associated with pulmonary fibrosis, osteopontin (OPN), in the stimulation of collagen-producing fibroblast proliferation, leading to fibrotic lesions.[23–25] While a number of factors during SWCNT exposure may contribute to the development of fibrotic lesions in lung tissue, both TGF-β1 and OPN have been reported to play a significant role in this particular model of pulmonary inflammation and fibrosis.[9,14,17,26]

TGF-β1 has been recognized as a central player in the robust pulmonary inflammatory response involved in the development of granulomas and interstitial fibrosis. TGF-β1 belongs to a superfamily of related pleiotropic growth factors that are important regulators of a variety of cellular processes such as cell growth, adhesion, migration, proliferation, differentiation, and apoptosis. It is a mitogenic factor for fibroblast differentiation into myofibroblasts[27] that mediates inflammatory responses, causes excess extracellular matrix (ECM) production and organization, increases tissue inhibitor of metalloproteinases (TIMP) synthesis, and decreases protease synthesis.[28] Previously, we have demonstrated that exposure of C57BL/6 mice to respirable SWCNT induced robust acute inflammation and increased level of TGF-β1 in lung lavage, ultimately causing a very early onset of pulmonary fibrosis and formation of granulomas.[8,9]

OPN, or secreted phosphoprotein 1 (*SPP1* gene), is a matricellular protein that acts as a matrix and chemotactic factor, which mediates diverse biological activities. OPN is secreted by activated T cells, macrophages, fibroblasts, and dendritic cells (DC). As a ligand, it interacts with a variety of receptor molecules, including thrombin, matrix metalloproteinases (MMPs), transmembrane proteins such as integrins and CD44, as well as ECM molecules, fibronectin, and collagen.[29,30] Importantly, OPN is required for granulomatous tissue formation in both infectious and non-infectious lung pathologies,[31–35] including giant foreign body cell formation.[36] OPN genes were reported to be significantly upregulated in rats exposed to SWCNT by intratracheal instillation through 365 days post-exposure and *Spp1* induction was recorded in bronchial epithelial cells during the observation period.[14]

Much less is known about the possible connections between OPN and TGF-β1 in pulmonary fibrosis. The aim of the study was to evaluate the importance of the OPN-TGF-β1 axis during the SWCNT-induced lung fibrotic response in mice. We hypothesized that OPN release contributes to total TGF-β1 production resulting in the increased collagen deposition observed during the formation of pulmonary fibrotic lesions. Thus we expected to see reduced lung injury and fewer fibrotic lesions in OPN-deficient mice due to hindered cytokine-cytokine interplay between OPN and TGF-β1. This study addresses the issue of relevant target biomolecules for therapeutics and prophylaxis in particle-induced and idiopathic pulmonary fibrosis.

Materials and methods

Particles

SWCNT (Unidym Inc., Sunnyvale CA) were produced by the high pressure CO disproportionation process (HiPco) technique and purified by acid treatment to remove metal contaminates. SWCNT were comprised of 99.7 wt% elemental carbon and 0.23 wt% iron. Comparative analytical data obtained by thermogravimetry/differential scanning calorimetry, temperature programmed oxidation, near infrared and Raman spectroscopy revealed that more than 99% of carbon content in the SWCNT HiPco product was accountable in a carbon nanotube morphology. Particles were deposited on polycarbonate filters and viewed under a field emission scanning electron microscope (SEM) (model S-4800; Hitachi, Tokyo, Japan). Although individual CNT fibers had diameter of 1–4 nm and a length of 100–1000 nm, they tended to form agglomerated bundles 1–3 μm in length and ~0.01 μm in width, thus having a high aspect ratio, but low rigidity. Surface area of the SWCNT 1040 m^2/g as measured by Brunauer, Emmett, and Teller (BET) analysis. Additionaly, more detailed information on characterization can be found elsewhere.[12]

Animals

Specific pathogen-free adult (8–10 weeks) female C57BL/6 mice (WT) and B6.129S6(Cg)-*Spp1*^{tm1Blh}/J osteopontin knockout mice (OPN-KO) were supplied by Jackson Lab (Bar Harbor, ME) and weighed 20.0 ± 1.6 g at the beginning of treatment. OPN KO mice were created through targeted disruption of the OPN gene in 129S6/SvEvTac derived mouse TL-1 embryonic stem cells. Successfully targeted cells were injected into C57BL6 blastocysts and the resulting chimeras crossed to outbred Black Swiss mice. Once established in this breed, heterozygotes were backcrossed for 10 generations with C57BL/6 mice. Animals were housed one per cage receiving HEPA-filtered air in the National Institute for Occupational Safety and Health (NIOSH) animal facilities accredited by AAALAC International. Animals were supplied with water and irradiated NIH-31 modified 6% mouse food (Envigo RMS, Inc.) *ad libitum* and were acclimated in the animal facility under controlled temperature and humidity for one week prior to use. All experimental procedures were conducted in accordance with the Guide for the Care and Use of Laboratory Animals, 7th ed. and approved by the National Institute for Occupational Safety and Health (NIOSH) Institutional Animal Care and Use Committee.

Administration of SWCNT

SWCNT stock suspension was prepared in Ca^{2+} and Mg^{2+}-free phosphate buffered saline (PBS) and sterilized by autoclaving. Levels of endotoxin were below the detection limit (0.01 EU/ml) as measured by a Limulus amebocyte lysate chromogenic endpoint assay kit (Hycult Biotech, Inc., Plymouth Meeting, PA). Samples were sonicated with a probe sonicator (Vibra Cell Sonics, 130 W, 20 kHz, 65% amplitude for 2 seconds) and immediately introduced into the mouse lung via pharyngeal aspiration. Briefly, the mice were anesthetized with a mixture of ketamine and xylazine (Phoenix, St. Joseph, MO) (41.65 and 1.65 mg/kg subcutaneous in the abdominal area) and secured against a board in a near upright position. The tongue was extended gently with forceps so that a 40 µl of SWCNT suspension (at a dose of 0 µg/mouse or 40 µg/mouse, 5 mice per study group) could be deposited in the caudal pharynx until aspirated into the lung. The corresponding control mice received sterile Ca^{2+} and Mg^{2+}-free PBS (40 µl) as a vehicle. A dose of 40 µg/mouse is relevant to occupational exposures and has been shown to produce significant fibrotic response upon pharyngeal aspiration in mice while not being able to overload the innate lung defense mechanisms.[4,8,37] All mice from both the control and treated groups survived the procedure and exhibited no overt behavioral or health outcomes. At 1, 7, and 28 days post exposure, mice were euthanized with an intraperitoneal injection of sodium phenobarbital (>100 mg/kg), weighed, and exsanguinated.

Obtaining bronchoalveolar lavage (BAL)

After exsanguination, the trachea was cannulated with a 22-gauge blunt needle and BAL was obtained by lavaging the lungs with 1.0 ml of ice-cold Ca^{2+} and Mg^{2+}-free PBS, for a recovery of approximately 0.5 ml (pool 1). Lungs were subsequently lavaged with 1.0 ml of ice-cold Ca^{2+} and Mg^{2+}-free PBS until a total of 5.0 ml (pool 2) was obtained. Cell pellets from both pools were recovered through centrifugation (800 × g, 10 min, 4 °C), combined, and resuspended in 0.5 ml of Ca^{2+} and Mg^{2+}-free PBS. Lactate dehydrogenase (LDH) measurements were performed in the acellular BAL from pool 1 while the remaining portion was aliquoted and stored at −80°C until further analysis of total proteins and cytokines.

Determining cell profiles of BAL fluids

In order to evaluate the degree of inflammatory response induced by the aspiration of SWCNT into the lung, recruitment of alveolar macrophages (AM), neutrophils, and lymphocytes recovered from BAL fluid were quantitated in relation to total cell count. Total amount of cells was counted using an electronic cell counter equipped with a cell sizing attachment (Coulter model Multisizer II with a 256C Channelizer; Coulter Electronics, Hialeah, FL). An additional cell suspension was cytocentrifuged onto a glass microscope slide (Shandon Cytospin 4; Thermo Fisher, Pittsburgh, PA). Centrifuge smears were stained with a Hema-3 kit (Fisher Scientific, Pittsburgh, PA) and differential cell counts were determined manually using light microscopy. Three hundred cells per slide were counted to achieve statistical significance.

Cytokine analysis in BAL

The release of TNF-α, IL-6, and MCP-1 was evaluated in the acellular BAL fluid at days 1, 7, and 28 following SWCNT exposures. Concentrations of TNF-α, IL-6, and MCP-1 (assay sensitivity of 7.3 pg/ml, 5 pg/ml, and 52.7 pg/ml respectively) were determined using a BD^{TM} Cytometric Bead Array, Mouse Inflammation kit (BD Biosciences, San Diego, CA) according to the manufacturer's protocol. Total TGF-β1 levels were measured using commercially available Multispecies Transforming Growth Factor-β1 ELISA kit (Biosource Intl. Inc.,).

Total protein and LDH activity in BAL

Measurement of total protein in the BAL fluid was performed by a modified Bradford assay according to the manufacturer's instructions (BioRad, Hercules, CA) with bovine serum albumin as a standard. Evaluation of LDH content is a formidable and one of the primary methods of pulmonary damage detection and assessment of pulmonary outcomes.[38,39] The activity of LDH was assayed spectrophotometrically by monitoring the reduction of NAD+ at 340 nm in the presence of lactate (Pointe Scientific, Inc., Lincoln Park, MI).

Collagen accumulation in the lung of SWCNT exposed OPN KO and WT mice

Total lung collagen content was determined by quantifying total soluble collagen using a Sircol Collagen Assay kit (Accurate Chemical and Scientific Corporation, Westbury, NY). Briefly, half of the lung was homogenized in 0.7 ml of 0.5 M acetic acid containing pepsin with 1:10 ratio of pepsin/tissue wet weight. Each sample was stirred vigorously for 24 hours at 4 °C, centrifuged, and 100 µl of supernatant was assayed according to the manufacturer's instructions (Accurate Chemical and Scientific Corporation, Westbury, NY).

Lung histopathology

Changes in lung morphology were analyzed by a board-certified pathologist at 7 and 28 days post exposure. Lungs were harvested, insufflated with 4% paraformaldehyde, coronal sections were cut from the lungs, embedded in paraffin, sectioned at a thickness of 5 µm with an HM 320 rotary microtome (Carl Zeiss, Thornwood, NY), stained with Masson trichrome, and submitted for histopathology. Slides were assessed for histopathologic changes, including the presence of pigment-laden macrophages, bronchiolar epithelial hyperplasia, peribronchial, perivascular and alveolar fibrosis, and the number of epithelioid granulomas. Sample identification was coded to ensure blinded evaluation.

Cell culture

RAW 264.7 murine macrophage cells were obtained from American Tissue Culture Collections (ATCC® TIB-71^{TM}) and murine lung epithelial cells (MLE-15) were a generous gift from Dr. Jeffrey A. Whitsett (Children's Hospital Medical Center, Cincinnati, OH). Cells were maintained in Dulbecco's Modified Eagle's Medium (DMEM) supplemented with 10% heat-inactivated fetal bovine serum (FBS), 100 units/ml penicillin, and 100 µg/ml streptomycin. Cell lines were seeded and exposed to four different concentrations of SWCNT (6 µg/cm^2–48 µg/cm^2 of monolayer surface) or control PBS and incubated for 24 hours at 37 °C in order to range-find the least cytotoxic concentration. For viability measurements cells were removed from the flasks using a solution containing 0.05% w/v trypsin and 0.5 mM EDTA (Invitrogen, Carlsbad,CA, USA), trypsin action was quenched after one minute by adding DMEM containing 5% FBS. Cells were centrifuged, washed twice and resuspended in PBS. 20-µl aliquot stained with an equal volume of 0.4% trypan blue (Invitrogen, San Diego, CA) was used to count cells with a hemocytometer to assess viability. The activity of LDH in culture supernatants was assayed spectrophotometrically as described previously.

Concentration of 12 µg/cm^2 was found to be non-cytotoxic for both cell types and was used for assessing the effect of OPN neutralization on TGF-β1 production. Concentrations of TGF-β1 (assay sensitivity of $<$ 15.6 pg/ml) and osteopontin (assay sensitivity of 5.7 pg/ml) in culture supernatants were determined using commercial ELISA kits (Biosource International Inc., Camarillo, CA and R&D Systems, Minneapolis, MN) with and without the presence of an OPN-blocking antibody (Sigma-Aldrich, St. Louis, MO). The cells were pretreated with blocking antibody 10 minutes

prior to the exposure at the concentration of 1 μg/ml. Bleomycin (0.1 μg/ml) was added to unexposed cells as a positive control. All cell-based experiments were repeated in triplicate.

Statistical analysis

Treatment related differences were evaluated using two-way ANOVA, followed by pair wise comparison using the Student-Newman-Keuls tests, as appropriate. Results are presented as the mean ± SEM. A p value less than 0.05 was considered statistically significant.

Results

Inflammatory cell recruitment elicited by pharyngeal aspiration of SWCNT

Upon administration, SWCNT elicited a typical robust and acute inflammatory response in WT mice after 1 day of exposure as evidenced by 175 fold increase in polymorphonuclear cells (PMNs) compared to control (Figure 1A). While OPN-KO also produced a significant influx of PMNs compared to control (100 fold increase), the results were significantly lower than in WT. By day 7, the response had diminished in both OPN-KO and WT mice. While PMN levels continued to remain low in WT mice, in OPN-KO mice they were significantly elevated compared to both its corresponding control and exposed WT counterpart by day 28. Following SWCNT exposure, macrophage recruitment revealed a slight time-dependent increase in OPN-KO mice (Figure 1B). However, in WT animals, macrophage recruitment peaked significantly at day 7 (1.5 fold), decreasing by day 28. We could see that SWCNT was phagocytosed by both WT and OPN KO alveolar macrophages in comparable quantities, and no particles were seen outside the cells in the BAL samples stained with hematoxylin-eosin at days 7 and 28. In contrast at 24 hours we observed both cells and free particle/agglomerates in the samples.

Pulmonary damage following SWCNT exposure

Following exposure, SWCNT induced pulmonary damage after 1 day as indicated by a significant increase in total protein levels relative to controls in both WT and OPN-KO mice in BAL fluid (145% and 135%) (Figure 2A). While both WT and OPN-KO animals exhibited pulmonary damage at a similar trend, decreased at 7 days and slightly elevated again at 28 days, only the WT remained significantly increased as compared to its corresponding control. Though the OPN-KO response paralleled that of WT mice, it was significantly less than in exposed WT counterparts at all time points after SWCNT instillation. Levels of tissue damage, as indicated by an increase in LDH release, were most prominent after 1 day of exposure in both WT and OPN-KO mice (225% and 150%) (Figure 2B). Similar to the response seen in protein levels, OPN-KO mice exhibited a more modest response when compared to its exposed WT counterpart at 1 day and

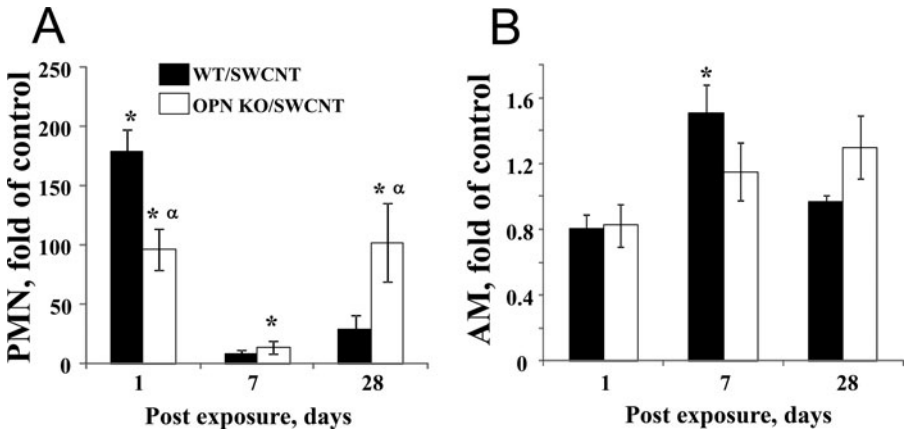

Figure 1. Cell differentials of bronchoalveolar lavage (BAL) fluid in C57BL6 (WT) and OPN-KO mice after pharyngeal aspiration of SWCNT (40 μg/mouse). **A: PMN** – polymorphonuclear cells. Mean absolute values from PBS-exposed WT mice were 1424.4 ± 406.9, 2585.8 ± 535.4, and 1393.5 ± 724.3 for 24 h, 7d and 28d respectively; from PBS-exposed OPN-KO mice: 901.6 ± 620.3, 1164.0 ± 490.1 and 859.2 ± 444.6 for 24 h, 7 d and 28 d respectively **B: AM** – alveolar macrophages. Mean absolute values from PBS-exposed WT mice were (601.4 ± 53.2) × 10^3, (492.1 ± 15) × 10^3, (621.2 ± 49.2 × 10) × 10^3 for 24 h, 7d and 28d respectively; from PBS-exposed OPN-KO mice (433.8 ± 30.3) × 10^3, (492.2 ± 39.8) × 10^3, (484.2 ± 51.9) × 10^3 for 24 h, 7d and 28d respectively. Values are expressed as Mean ± SEM. * $p < 0.05$ vs. PBS-exposed WT mice, $^{\alpha}$ $p < 0.05$ vs. WT mice exposed to SWCNT.

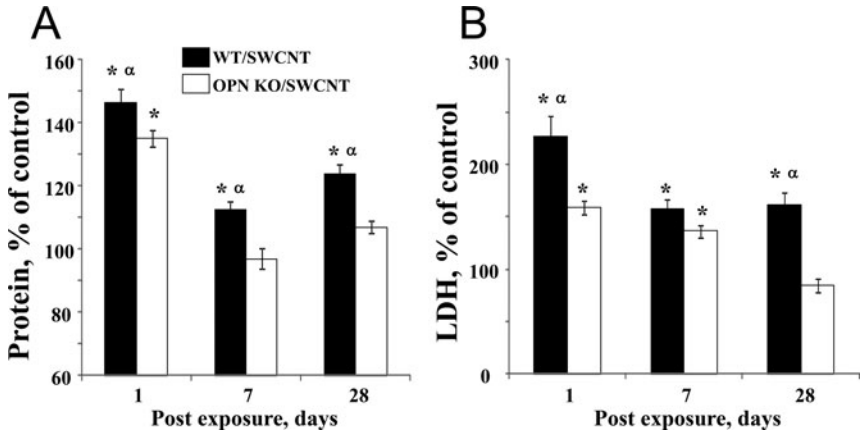

Figure 2. Pulmonary cell damage as indicated by changes in levels of protein and release of lactate dehydrogenase (LDH) in bronchoalveolar lavage (BAL) fluid in C57BL6 (WT) and OPN-KO mice after pharyngeal aspiration of SWCNT (40 μg/mouse). **A:** Total protein. **B:** LDH. Values are expressed as mean ± SEM. * $p < 0.05$ vs. control mice, $^{\alpha}$ $p < 0.05$ vs. OPN-KO mice exposed to SWCNT.

28 day post exposure. While these levels decreased more rapidly by day 7 in WT animals, the response remained significantly elevated at all time points compared to its controls. Levels did not begin to diminish until day 28 for OPN-KO mice.

Pro-inflammatory cytokine production in C57/BL6 and OPN-Deficient mice

In both OPN-KO and WT mice, an increase of pro-inflammatory pulmonary cytokines concentrations was observed in the BAL following 1 day post exposure to SWCNT, compared to controls (Figure 3A, B, C), with the magnitude of TNF-α, IL-6, and MCP-1 secretion consistently lower in OPN-KO mice. Differences in pro-inflammatory cytokine profiles for both OPN-KO and WT mice faded by day 7.

TGF-β1 release in BAL of C57BL/6 and OPN-Deficient mice

Following exposure in WT mice, TGF-β1 release peaked significantly on day 7 (2.3 fold of control) and subsequently diminished by day 28 (Figure 4A). In OPN-KO animals, TGF-β1 release was not significantly elevated in BAL at any time point and only increased slightly over time.

Collagen accumulation at 28 days after SWCNT exposure

To investigate the level of fibrosis induced by SWCNT in OPN-KO and WT mice, the accumulation of collagen in the lung was assessed at day 28 post-exposure. Collagen levels were significantly increased in WT animals with normal OPN expression (180% of control) compared to OPN-KO mice, which did not differ from its controls. (Figure 4B).

Pathology of lung tissue from OPN-KO and WT mice

Microscopic evaluation of the lungs of mice in control groups reveals normal morphology of conducting and respiratory airways (Figure 5A). Lungs of C57BL6 mice exposed to SWCNT at 7 and 28 days revealed

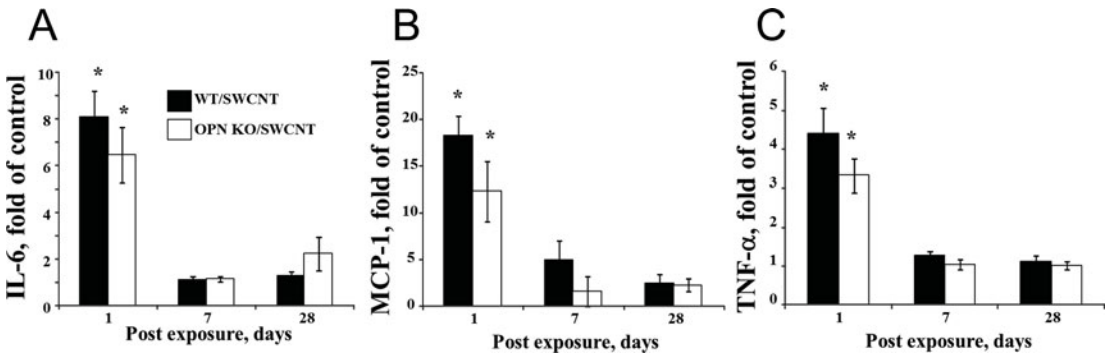

Figure 3. Inflammatory cytokine release in bronchoalveolar lavage (BAL) fluid in C57BL6 (WT) and OPN-KO mice after pharyngeal aspiration of SWCNT (40 μg/mouse). **A.** IL-6. **B:** MCP-1. **C.** TNF-α. Values are expressed as mean ± SEM. * $p < 0.05$ vs. control mice.

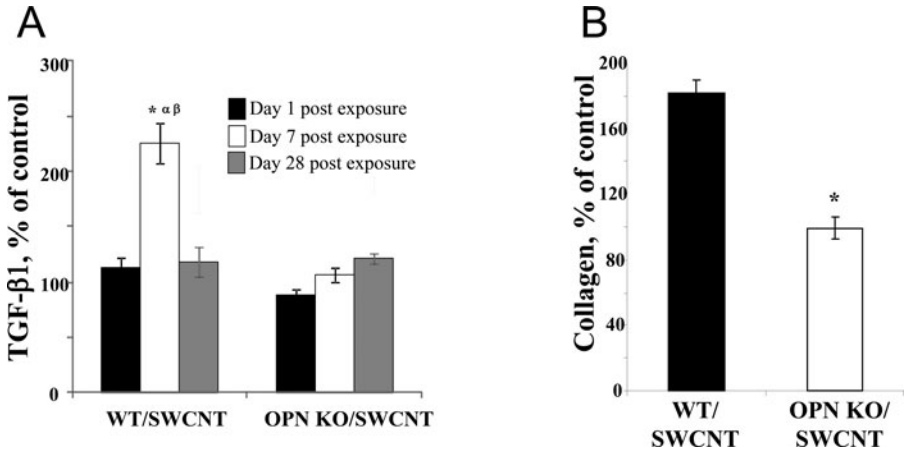

Figure 4. TGF-β release in bronchoalveolar lavage (BAL) fluid and collagen deposition in the lung of C57BL6 (WT) and OPN-KO mice after pharyngeal aspiration of SWCNT (40 μg/mouse). **A.** TGF-β release as measured in mice sacrificed at 24 hours (black columns), 7 days (white columns), and 28 days (gray columns). **B.** Collagen deposition in the lung as measured in mice sacrificed at 28 days post exposure. Values are expressed as mean ± SEM. * $p < 0.05$ vs. PBS-exposed WT mice. $^{\alpha}$ $p < 0.05$ vs. OPN-KO mice exposed to SWCNT 7 days post exposure. $^{\beta}$ $p < 0.05$ vs. WT mice exposed to SWCNT 1 day post exposure. $^{\gamma}$ $p < 0.05$, vs WT mice exposed to SWCNT.

deposition of brown pigmented particles in small airways and numerous epithelioid granulomas composed of pigment-laden macrophages (Fig. B and C). The average number of granulomas: 6.6 per 10 high-power fields (HPF) at 7 days, 7.5 per 10 HPF at 28 days. There was minimal alveolar fibrosis associated with granulomas. No significant interstitial lymphocytic infiltration, epithelial hypertrophy/hyperplasia, goblet cell hyperplasia, or features of airway remodeling was seen. Lungs of OPN-KO mice exposed to SWCNT at 7 and 28 days (Fig. E and F) revealed similar histologic findings, however, the number of granulomas was significantly reduced: 1.4 per 10 HPF at 7 days, 3.7 per 10 HPF at 28 days. No fibrosis was seen. Overall, the lungs of OPN-KO mice were significantly less affected by SWCNT exposure compared to WT.

In vitro *RAW 264.7 macrophages and MLE-15 exposure to SWCNT*

Two cell types, RAW 264.7 Macrophages (MΦ) and alveolar epithelial cells (MLE-15), were exposed for 24 hours to SWCNT concentrations ranging from 6 μg/cm^2 to 48 μg/cm^2. The viability of RAW 264.7 MΦ decreased in a dose-dependent manner, although cells exposed to 6 and 12 μg/cm^2 did not vary significantly from controls. A similar trend was observed in MLE-15 cells, though this viability decrease was not as rapid; however, all cells exposed to a dose greater than or equal to 12 μg/cm^2 differed significantly from controls (Figure 6A). As expected, the lowest viability for both cell lines was observed at the highest concentration of SWCNT (48 μg/cm^2). LDH release in RAW 264.7 MΦ showed a significant dose dependent increase while LDH measured in MLE-15 cells was nearly dose-dependent (a slight decrease was measured at 24 μg/cm^2 relative to 12 μg/cm^2) (Figure 6B).

Following SWCNT exposure (12 μg/cm^2), significantly higher levels of OPN content were observed, 158.5% and 132.6%, compared to controls of RAW 264.7 MΦ and MLE-15 conditioned supernatants, respectively (Figure 7A, **8A**). SWCNT-exposed cells also demonstrated increased TGF-β1 content, 163.9%, and 143.8%, compared to respective controls for RAW 264.7 MΦ and MLE-15 cells (Figure 7B, 8B). With the addition of mouse anti-OPN antibody in neutralizing concentration, we observed inhibition of OPN secretion in response to SWCNT exposure in cell supernatants, as expected. Inhibition of OPN production reduced the levels of TGF-β1 compared to that of cells treated only with SWCNT. Exposure to SWCNT in the presence of OPN blocking antibody caused significantly less TGF-β1 release in RAW 264.7 MΦ, but not in MLE-15 cells.

Discussion

As occupational exposure to nanoparticles increases due to a large demand for nanomaterials in consumer products, the human health risks involved must also be evaluated. Specifically, the relevance of SWCNT exposure to the development of pulmonary inflammation and interstitial fibrosis resembling that of IPF, though

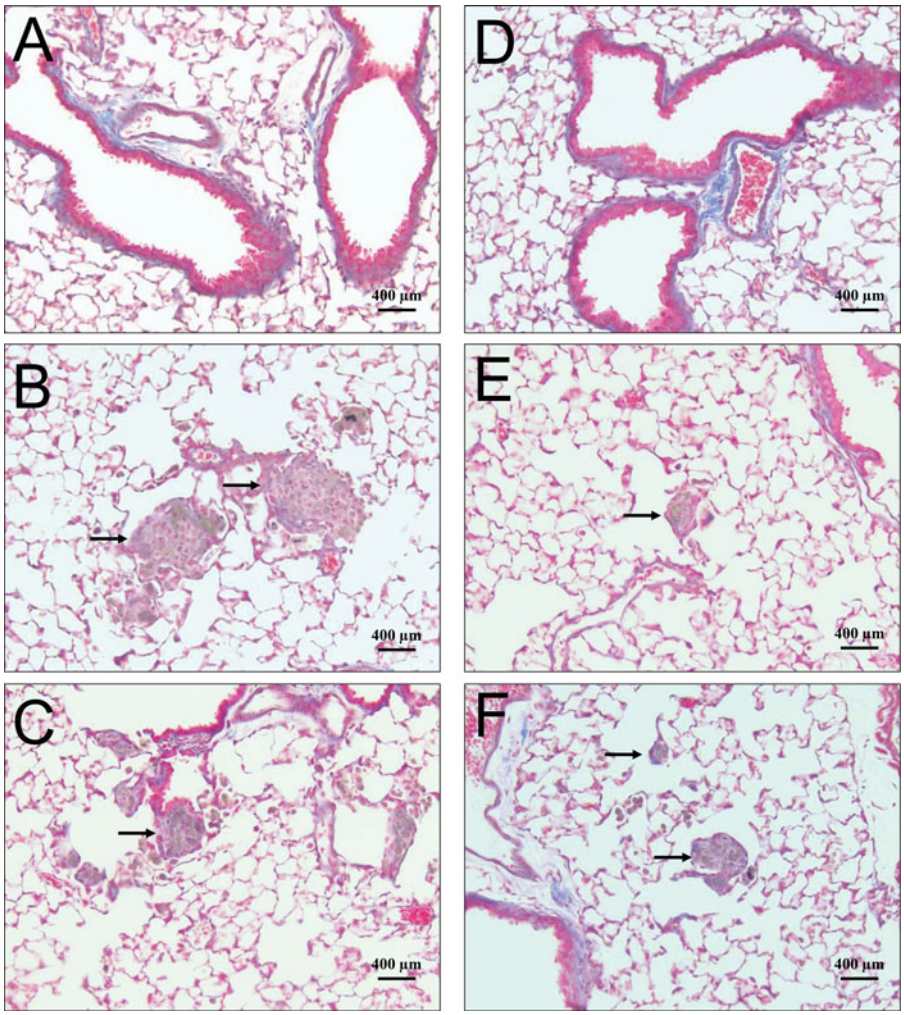

Figure 5. Representative photomicrographs of lung tissue from C57BL6 (WT) and OPN-KO mice administered PBS (Control) or SWCNT (40 µg/mouse). Granulomas are indicated by the black arrows. **A**: Lung tissue from a control WT mouse sacrificed at 7 days. Lung exhibits normal morphology and no lesions are present. **B**: Lung tissue from SWCNT-exposed WT mouse sacrificed at 7 days. **C**: Lung tissue from SWCNT-exposed WT mouse sacrificed at 28 days. The tissue contains large granulomas, containing pigmented particulate matter. **D**: Lung tissue from a control OPN-KO mouse sacrificed at 7 days. Lung exhibits normal morphology and no lesions are present. **E**: Lung tissue from SWCNT exposed OPN-KO mouse sacrificed at 7 days. **F**: Lung tissue from SWCNT exposed OPN-KO mouse sacrificed at 28 days.

well researched, warrants an investigation into the possible mechanisms leading to these disease states.

So far, several pathophysiological mechanisms responsible for the CNT-induced fibrosis have been proposed. A major contributor to SWCNT-induced fibrosis are stem-like fibroblasts and fibroblasts originating from epithelial-mesenchimal transition (EMT) process, that are fully functional in terms of collagen production.[40–42] Production of reactive oxygen species (ROS) by SWCNT upregulates TGF-β1 expression,[41] which in turn further stimulates collagen production, ECM organization, induces EMT, promotes the fibroblast to myofibroblast differentiation, and induces contractive activity in myofibroblasts. TGF-β/p-Smad2 and β-catenin pathways activation in hyperplastic epithelial cells is thought to contribute to EMT and fibroblast population expansion. Overall, TGF-β1 inducing effects of CNT on individual cell types are well summed up in a recent review.[43]

OPN expression was found to be significantly upregulated upon exposure to SWCNT similar to that observed for MWCNT.[14,17,26] CNT exposure, being an initial insult, activates the secretion of several cytokines by AM and recruitment of additional macrophages and T-lymphocytes. MMPs produced by macrophages proteolytically cleave OPN and its fragments may in turn bind to integrins, inducing cell adhesion molecules expression and promoting the formation of granulomatous lesions.[44,45] Importantly, OPN provides survival signals in fibroblasts;

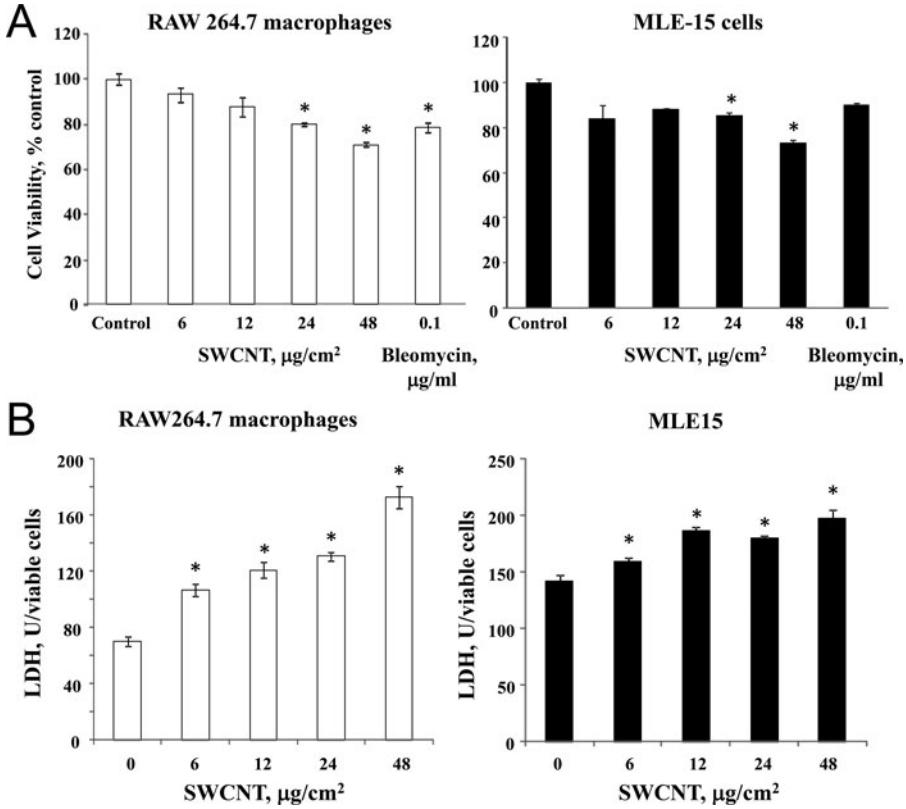

Figure 6. Viability (**A**) and LDH release (**B**) of RAW 264.7 macrophages and MLE-15 cells following 24 hour exposure of SWCNT (6–48 μg/cm^2). Values are expressed as mean ± SEM. *$p < 0.05$ vs. control mice.

its absence leads to caspase-independent necrosis,[46] contributes to local Th17 differentiation in pulmonary fibrosis,[47] and induces mesenchymal stem cells migration.[48] OPN was even named "A Master Regulator of Epithelial-Mesenchymal Transition" through Twist, ZEB and Snail pathways in a recent paper.[49]

A potential modulating mechanism is speculated to exist between OPN and TGF-β1 due to their fundamental role in mediating fibrosis. Indeed, TGF-β1 treatment has been shown to upregulate OPN secretion in fibroblasts.[50] Mechanistically, it can activate the OPN promoter via the Hox-binding element,[51] but there is controversy as to the Smad4 (downstream

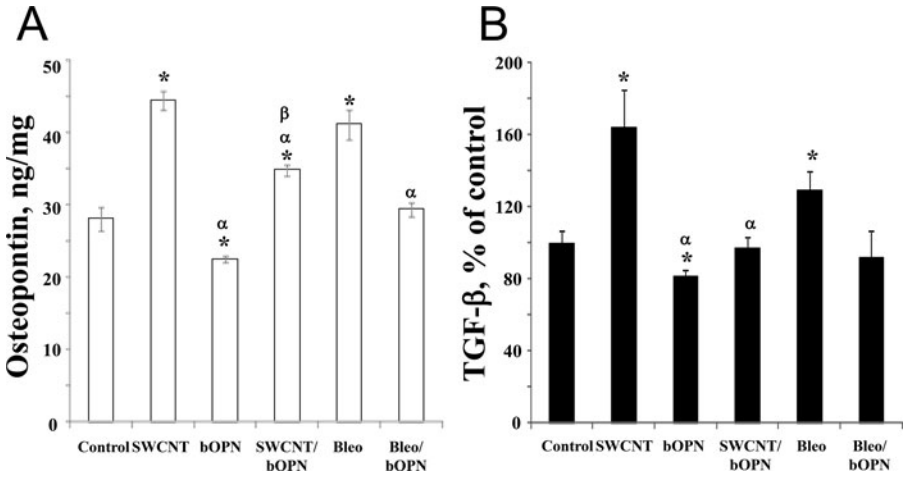

Figure 7. Osteopontin accumulation (**A**) and TGF-β1 release (**B**) in supernatants of RAW 264.7 macrophages following 24 hour exposure of SWCNT (12 μg/cm^2) and in the presence of an anti-OPN antibody (bOPN, 1 μg/ml). *$p < 0.05$ *vs*. control cells; $^{\alpha}$ $p < 0.05$ *vs*. SWCNT only exposed cells; $^{\beta}$ $p < 0.05$ *vs*. bOPN only exposed cells.

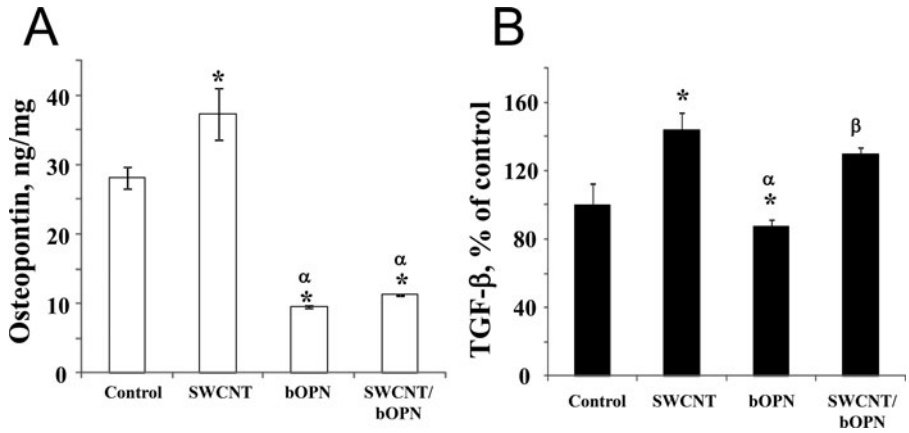

Figure 8. Osteopontin accumulation (**A**) and TGF-β1 release (**B**) in supernatants of MLE-15 cells following 24 hour exposure of SWCNT (12 μg/cm^2) and in the presence of an anti-OPN antibody (1 μg/ml). *p < 0.05 *vs*. control cells; $^{\alpha}$ p < 0.05 *vs*. SWCNT only exposed cells; $^{\beta}$ p < 0.05 *vs*. bOPN only exposed cells.

signaling molecule in TGF-β1 pathway) function – it has been shown to de-repress the *OPN* gene promoter in lung epithelial (Mv1Lu) cells[52] and suppress *OPN* gene in A549 cells.[52] It seems that OPN is likely to be differentially regulated by TGF-β1 in multiple cell types. OPN may also act upstream of TGF-β1 in certain conditions. OPN is required for TGF-β1 to stimulate α-smooth muscle actin, extradomain-A and connective tissue growth factor.[53] OPN induces MMP-9 expression,[54,55] which in turn is an activator of TGF-β1.[45] A recent study has shown the induction of TGF-β1 expression in mesenchymal stem cells by OPN through myeloid zinc finger 1 (MZF1).[56,57]

Despite this, we lack any reliable data on OPN–TGF-β1 cross-talk and though studies of the fibrotic role of these proteins are extensive, the functions of OPN during particulate-induced inflammation and its subsequent interplay with TGF-β1 is largely unknown. Due to the important role of OPN and TGF-β1 in inducing formation of fibrosis and wound healing, we hypothesized that exposure to SWCNT in an OPN-deficient mouse model would decrease the overall collagen deposition and fibrotic response in OPN-deficient mice in part due to hindered cytokine-cytokine interplay. In order to investigate this, C57BL/6 and OPN-deficient were administered SWCNT through pharyngeal aspiration and the resulting pulmonary damage and inflammatory responses were analyzed. Previous pharyngeal aspiration studies provided reliable particle delivery to deep lung regions and to be highly correlated with the administered dose.[8,58] To further address the issue, RAW 264.7 macrophages and murine lung epithelial cells (MLE-15) were exposed to SWCNT or bleomycin (as it has been shown to increase TGF-β1 expression[59]), for 24 hours with and without the presence of an OPN-blocking antibody.

Exposure of OPN-KO mice to SWCNT over the course of 28 days revealed a slight increase in TGF-β1 release, which did not significantly change at any time point. However, in WT mice, a significant increase in TGF-β1 was observed at 7 days, which diminished by day 28. Further investigation into the inflammatory response of OPN-KO mice revealed notable differences when compared to WT. Previously, we have demonstrated that exposure to SWCNT results in early neutrophil accumulation accompanied by elevated levels of pro-inflammatory cytokines at 1 day post exposure, followed by an influx of macrophage recruitment and a peak in release of TGF-β1 levels occurring by day 7.[89] In this study, our results are consistent in the WT model, demonstrating a similar time course of TNF-α, IL-6, and MCP-1 release corresponding to an influx of neutrophils, whereas TGF-β1 release paralleled macrophage recruitment (Figure 5, Figure 1). These activated macrophages normally accumulate at the sites of injury and release growth factors, such as PDGF, OPN, and TGF-β1, which stimulate the proliferation and migration of collagen-producing fibroblasts to induce granulomas formation.[24,60,61] In addition, we observed numerous foci of particle-laden alveolar macrophages forming distinct granulomas associated with alveolar fibrosis in the lungs of WT mice, as well as an accumulation of collagen by day 28 (Figure 5, Figure 4B). However, in OPN-KO mice, though the release of pro-inflammatory cytokines in BAL also corresponded to its influx of neutrophils,

these levels were markedly reduced, for the most part, compared to WT counterpart (Figure 3A, B, C). This supports previous studies indicating the role of OPN as a chemotactic cytokine for macrophages, dendritic cells, and neutrophils through engagement of CD44 and integrin receptors, revealing reduced PMN chemotaxis in OPN deficient mice.[62,63] This lessened neutrophil accumulation in turn may also lead to a reduction of overall TGF-β1 production.[64,65] Although PMNs were elevated at day 28 in OPN-KO mice, there appeared to be no significant elevation in pro-inflammatory cytokines. There was no statistically significant increase in AM influx at all timepoints in exposed OPN-KO mice compared to control. Studies by O'Regan et al. and Ophascharoensuk et al. have suggested impaired injury-induced AM recruitment in OPN-deficient mice, and OPN-null macrophages show markedly decreased migration abilities towards MCP-1 and fMLP and are more likely to enter the apoptosis.[35,66] On the contrary, several previous studies reported normal AM recruitment[30,34] in OPN-deficient animals, although in tuberculosis rather than particle-induced model. Nonetheless, in our study, no significant alterations were observed in AM accumulation between OPN-KO and WT mice upon exposure to SWCNT. It appears that SWCNT are more likely to be recognized by macrophages in more agglomerated form, rather than highly dispersed,[4] so the granuloma formation in WT mice was likely to occur not only due to high penetration retention period, but also due to the inability to get rid of the aspirated particulates despite being recognized and engulfed by phagocytes, while OPN deficiency could abrogate the granuloma formation itself.

Overall, the severity of pulmonary cell damage was reduced in the OPN-deficient mouse model, as indicated by total protein and LDH levels in BAL (Fig. 2). The overall number and severity of granulomas as well as a collagen accumulation in the lungs of OPN KO mice were markedly decreased, (Figure 4B). Taken together, these results support previous findings indicating the important role of OPN in SWCNT-induced alterations. A number of studies have found a reduction of collagen deposition, fibrosis and scarring in other tissues, such as myocardium, kidneys, liver, ureter and skin via OPN neutralization or in OPN -/- animals.[67–72]

Previously, we have demonstrated that production of TGF-β1 in RAW 264.7 macrophages was induced by SWCNT exposure[9] and in the study by Wu et al. OPN$^{-/-}$ murine bone-marrow derived macrophages displayed reduced basal production of TGF-β1.[71] Additionally, in a recent paper implementing an adverse outcome pathway analysis, macrophages exposed to CNT are proposed to act as paracrine signalers for the activation of fibroblasts through growth factors and OPN production.[43] Thus, in order to supplement our *in vivo* study, a set of separate *in vitro* experiments using RAW 264.7 rat macrophages and MLE-15 cells was conducted. The resulting data was concurrent with previous findings, revealing an increase in OPN accumulation, TGF-β1 release, and damage (as indicated by LDH release) when exposed to SWCNT (Figure 6, 7, 8). It was also revealed that in the presence of an OPN-blocking antibody, SWCNT-induced TGF-β1 release in RAW 264.7 supernatants was significantly less than those cells exposed to SWCNT and isotype control antibodies, while MLE-15 cells exhibited insignificant decrease in TGF- β1.

Though our results have indicated a clear association between the two cytokines involved in SWCNT-induced pulmonary fibrotic response initiation and progression, the exact mechanisms through which these two interact remain unclear, although several theories arise from the previously published results. The OPN deficient animals have been shown to exhibit decreased oxidative stress in several conditions related to the inflammatory response and fibrotic processes.[73,74] This might explain the decreased cytokine secretion, while decreased ROS production by immune cells could've affected the activation of TGF-β1. SWCNTs, in particular, have been shown to act through AP-1 transcription factor activation,[75] which is responsible for both TGF-β1 and OPN activation and modulation.[76,77] In myocardial fibrosis AP-1 activation is dependent on OPN stimulation[78] and this transcription factor was also downregulated in OPN-KO mice upon pulmonary asbestos exposure.[79]

Since only a small amount of TGF-β1 is diffusible, cell-cell interactions play a major role in its activation.[80] The absence of OPN leads to a distinct reduction of those cell-cell interactions due to the fact that OPN-null cells have less contractility and lowered adhesion.[53] Failure to restore epithelial basement membrane integrity is a key step in promoting fibrosis (as epithelial cells may interact with mesenchymal cells),[81] in the OPN-KO animals this mechanism might be abrogated. The anti-apoptotic

activity of OPN[46,82] is crucial for continuous activity of macrophages and fibroblasts at the sites of injury, since in both cell types SWCNT and MWCNT specifically upregulate the expression of TGF-β1,[21,83–85] TGF-β receptor 1 and Smad2/3.[21] As OPN-deficient animals exhibit reduced Th17 differentiation of CD4+ $\alpha\beta$ T cells and IL-17-producing $\gamma\delta$ T cells,[47] decrease in IL-17 induced TGF-β1 production also seem to be a feasible mechanism.

One should also consider the other important mechanisms and cytokine interactions involved in the pulmonary fibrosis induction and progression, such as combined action of PDGF and TGF-β1.[61] PDGF itself, which was found to be upregulated in SWCNT-treated animals,[26] also participates in upregulating the expression of OPN[86,87] and may implement its action in part through the OPN promotion, which has been shown for the smooth muscle cells.[88,89] There's little data as of yet regarding the possible OPN upstream effects on PDGF signaling, but interestingly, one of the recent papers describes the hampering of Focal adhesion kinase (FAK) phosphorylation by PDGF in osteoblasts and fibroblasts upon the recombinant OPN treatment,[90] thus potentially reducing their migration activity. This is an interesting mechanism, which might be a part of negative feedback in the regulation of fibrogenesis and needs further investigation.

Our study harbors a number of limitations that need to be mentioned. Firstly, although the use of the knockout mouse model proved to be a valuable tool for the specific toxicity investigations, results will be hard to extrapolate to human pathology due to the fact that alterations to genome may have unexpected side effects in the particular exposure model, i.e. the intracellular OPN (iOPN) expression, which has to be addressed in future experiments. Also, for the *in vitro* proof of concept experiment, rather than follow the pulmonary exposure equivalence principle, we used the highest least cytotoxic dose of 12 μg/cm^2 of SWCNT when assessing the effect of OPN neutralization on TGF-β1 production. Several studies have shown that in the long run some biological effects, including induction of proliferation and even malignant transformation may occur at doses as low as 0.02 μg/cm^2.[91,92]

In our study OPN-KO mice developed distinctly decreased granulomatous lesions formation and much less collagen deposition upon exposure to SWCNT in lung fibrosis-promoting doses while TGF-β1 levels in BAL remained unchanged. Murine RAW 264.7, but not MLE-15 cells treated with SWCNT had significantly less TGF-β1 released in the presence of OPN-blocking antibody. In summary, we conclude that OPN might be important in initiating the cellular mechanisms that produce an overall response in SWCNT model of pulmonary fibrosis, occurring upstream of TGF-β1 signaling. Lower number of granulomas, containing fewer characteristic macrophages in OPN-KO mice and *in vitro* study results point at macrophages as one of the more conceivable players. A recent study has shown that in MWCNT it is possible to reduce the OPN expression and pulmonary fibrosis in mice by coating the nanotubes with aluminum oxide,[93] but whether SWCNT could be treated for the same effect is not known. Further investigations into the OPN/integrins axis, OPN-linked gene expression, MSC migration and collagen fibrillogenesis is needed to better predict and determine the TGF-β1 mediated pulmonary fibrosis outcomes and to target the mediator molecules involved in OPN-TGF-β1 interplay.

Declaration of interests

Authors declare no conflict of interests.

Disclaimer

The findings and conclusions in this report are those of the authors and do not necessary represent the view of the National Institute for Occupational Safety and Health policy.

All experimental procedures were approved by the National Institute for Occupational Safety and Health Institutional Animal Care and Use Committee.

Funding

This project is funded by National Institute for Occupational Safety and Health ID: NORA 939051G.

References

1. De Volder MFL, Tawfick SH, Baughman RH, Hart AJ. Carbon Nanotubes: Present and Future Commercial Applications. *Science*. 2013;339(6119):535–9.
2. Vance ME, Kuiken T, Vejerano EP, McGinnis SP, Hochella MF, Jr., Rejeski D, et al. Nanotechnology in the real world: Redeveloping the nanomaterial consumer products inventory. *Beilstein J Nanotechnol*. 2015;6:1769–80.
3. McWilliams A. Global Markets for Nanocomposites, Nanoparticles, Nanoclays, and Nanotubes. BCC Research Inc; 2017. www.bccresearch.com.
4. Mercer RR, Scabilloni J, Wang L, Kisin E, Murray AR, Schwegler-Berry D, et al. Alteration of deposition

pattern and pulmonary response as a result of improved dispersion of aspirated single-walled carbon nanotubes in a mouse model. *Am J Physiol Lung Cell Mol Physiol*. 2008;294(1):L87–97.
5. Murray AR, Kisin ER, Tkach AV, Yanamala N, Mercer R, Young SH, et al. Factoring-in agglomeration of carbon nanotubes and nanofibers for better prediction of their toxicity versus asbestos. *Part Fibre Toxicol*. 2012;9:10.
6. Park EJ, Roh J, Kim SN, Kang MS, Han YA, Kim Y, et al. A single intratracheal instillation of single-walled carbon nanotubes induced early lung fibrosis and subchronic tissue damage in mice. *Arch Toxicol*. 2011;85(9):1121–31.
7. Shvedova AA, Fabisiak JP, Kisin ER, Murray AR, Roberts JR, Tyurina YY, et al. Sequential exposure to carbon nanotubes and bacteria enhances pulmonary inflammation and infectivity. *Am J Respir Cell Mol Biol*. 2008;38(5):579–90.
8. Shvedova AA, Kisin E, Murray AR, Johnson VJ, Gorelik O, Arepalli S, et al. Inhalation vs. aspiration of single-walled carbon nanotubes in C57BL/6 mice: inflammation, fibrosis, oxidative stress, and mutagenesis. *Am J Physiol Lung Cell Mol Physiol*. 2008;295(4):L552–65.
9. Shvedova AA, Kisin ER, Mercer R, Murray AR, Johnson VJ, Potapovich AI, et al. Unusual inflammatory and fibrogenic pulmonary responses to single-walled carbon nanotubes in mice. *Am J Physiol Lung Cell Mol Physiol*. 2005;289(5):L698–708.
10. Shvedova AA, Kisin ER, Murray AR, Gorelik O, Arepalli S, Castranova V, et al. Vitamin E deficiency enhances pulmonary inflammatory response and oxidative stress induced by single-walled carbon nanotubes in C57BL/6 mice. *Toxicol Appl Pharmacol*. 2007;221(3):339–48.
11. Shvedova AA, Kisin ER, Murray AR, Kommineni C, Castranova V, Fadeel B, et al. Increased accumulation of neutrophils and decreased fibrosis in the lung of NADPH oxidase-deficient C57BL/6 mice exposed to carbon nanotubes. *Toxicol Appl Pharmacol*. 2008;231(2):235–40.
12. Shvedova AA, Yanamala N, Kisin ER, Tkach AV, Murray AR, Hubbs A, et al. Long-term effects of carbon containing engineered nanomaterials and asbestos in the lung: one source postexposure comparisons. *Am J Physiol Lung Cell Mol Physiol*. 2014;306(2):L170–82.
13. Teeguarden JG, Webb-Robertson BJ, Waters KM, Murray AR, Kisin ER, Varnum SM, et al. Comparative proteomics and pulmonary toxicity of instilled single-walled carbon nanotubes, crocidolite asbestos, and ultrafine carbon black in mice. *Toxicol Sci*. 2011;120(1):123–35.
14. Fujita K, Fukuda M, Fukui H, Horie M, Endoh S, Uchida K, et al. Intratracheal instillation of single-wall carbon nanotubes in the rat lung induces time-dependent changes in gene expression. *Nanotoxicology*. 2015;9(3):290–301.
15. Mutlu GM, Budinger GR, Green AA, Urich D, Soberanes S, Chiarella SE, et al. Biocompatible nanoscale dispersion of single-walled carbon nanotubes minimizes in vivo pulmonary toxicity. *Nano Lett*. 2010;10(5):1664–70.
16. Lam CW, James JT, McCluskey R, Hunter RL. Pulmonary toxicity of single-wall carbon nanotubes in mice 7 and 90 days after intratracheal instillation. *Toxicol Sci*. 2004;77(1):126–34.
17. Huizar I, Malur A, Midgette YA, Kukoly C, Chen P, Ke PC, et al. Novel murine model of chronic granulomatous lung inflammation elicited by carbon nanotubes. *Am J Respir Cell Mol Biol*. 2011;45(4):858–66.
18. Sturm R Clearance of carbon nanotubes in the human respiratory tract-a theoretical approach. *Ann Transl Med*. 2014;2(5):46.
19. Mercer RR, Hubbs AF, Scabilloni JF, Wang L, Battelli LA, Friend S, et al. Pulmonary fibrotic response to aspiration of multi-walled carbon nanotubes. *Part Fibre Toxicol*. 2011;8:21.
20. Konduru NV, Tyurina YY, Feng W, Basova LV, Belikova NA, Bayir H, et al. Phosphatidylserine targets single-walled carbon nanotubes to professional phagocytes in vitro and in vivo. *PLoS One*. 2009;4(2):e4398.
21. Mishra A, Stueckle TA, Mercer RR, Derk R, Rojanasakul Y, Castranova V, et al. Identification of TGF-beta receptor-1 as a key regulator of carbon nanotube-induced fibrogenesis. *Am J Physiol Lung Cell Mol Physiol*. 2015;309(8):L821–33.
22. Luanpitpong S, Wang L, Manke A, Martin KH, Ammer AG, Castranova V, et al. Induction of stemlike cells with fibrogenic properties by carbon nanotubes and its role in fibrogenesis. *Nano Lett*. 2014;14(6):3110–6.
23. Khalil N, O'Connor RN, Unruh HW, Warren PW, Flanders KC, Kemp A, et al. Increased production and immunohistochemical localization of transforming growth factor-beta in idiopathic pulmonary fibrosis. *Am J Respir Cell Mol Biol*. 1991;5(2):155–62.
24. Kogan EA, Tyong FV, Demura SA. [The mechanism of lung tissue remodeling in the progression of idiopathic pulmonary fibrosis]. *Arkh Patol*. 2010;72(4):30–6.
25. Ma JY, Mercer RR, Barger M, Schwegler-Berry D, Scabilloni J, Ma JK, et al. Induction of pulmonary fibrosis by cerium oxide nanoparticles. *Toxicol Appl Pharmacol*. 2012;262(3):255–64.
26. Mangum JB, Turpin EA, Antao-Menezes A, Cesta MF, Bermudez E, Bonner JC. Single-walled carbon nanotube (SWCNT)-induced interstitial fibrosis in the lungs of rats is associated with increased levels of PDGF mRNA and the formation of unique intercellular carbon structures that bridge alveolar macrophages in situ. *Part Fibre Toxicol*. 2006;3:15.
27. Kaarteenaho-Wiik R, Sademies O, Paakko P, Risteli J, Soini Y. Extracellular matrix proteins and myofibroblasts in granulomas of sarcoidosis, atypical mycobacteriosis, and tuberculosis of the lung. *Hum Pathol*. 2007;38(1):147–53.
28. Wipff PJ, Hinz B. Integrins and the activation of latent transforming growth factor beta1 – an intimate relationship. *Eur J Cell Biol*. 2008;87(8–9):601–15.
29. Giachelli CM, Lombardi D, Johnson RJ, Murry CE, Almeida M. Evidence for a role of osteopontin in

macrophage infiltration in response to pathological stimuli in vivo. *Am J Pathol*. 1998;152(2):353–8.
30. Liaw L, Birk DE, Ballas CB, Whitsitt JS, Davidson JM, Hogan BL. Altered wound healing in mice lacking a functional osteopontin gene (spp1). *J Clin Invest*. 1998;101(7):1468–78.
31. Ashkar S, Weber GF, Panoutsakopoulou V, Sanchirico ME, Jansson M, Zawaideh S, et al. Eta-1 (osteopontin): an early component of type-1 (cell-mediated) immunity. *Science*. 2000;287(5454):860–4.
32. Morimoto J, Inobe M, Kimura C, Kon S, Diao H, Aoki M, et al. Osteopontin affects the persistence of beta-glucan-induced hepatic granuloma formation and tissue injury through two distinct mechanisms. *Int Immunol*. 2004;16(3):477–88.
33. Nau GJ, Guilfoile P, Chupp GL, Berman JS, Kim SJ, Kornfeld H, et al. A chemoattractant cytokine associated with granulomas in tuberculosis and silicosis. *Proc Natl Acad Sci U S A*. 1997;94(12):6414–9.
34. Nau GJ, Liaw L, Chupp GL, Berman JS, Hogan BL, Young RA. Attenuated host resistance against Mycobacterium bovis BCG infection in mice lacking osteopontin. *Infect Immun*. 1999;67(8):4223–30.
35. O'Regan AW, Hayden JM, Body S, Liaw L, Mulligan N, Goetschkes M, et al. Abnormal pulmonary granuloma formation in osteopontin-deficient mice. *Am J Respir Crit Care Med*. 2001;164(12):2243–7.
36. Tsai AT, Rice J, Scatena M, Liaw L, Ratner BD, Giachelli CM. The role of osteopontin in foreign body giant cell formation. *Biomaterials*. 2005;26(29):5835–43.
37. Rydman EM, Ilves M, Vanhala E, Vippola M, Lehto M, Kinaret PA, et al. A Single Aspiration of Rod-like Carbon Nanotubes Induces Asbestos-like Pulmonary Inflammation Mediated in Part by the IL-1 Receptor. *Toxicol Sci*. 2015;147(1):140–55.
38. Drent M, Cobben NA, Henderson RF, Wouters EF, van Dieijen-Visser M. Usefulness of lactate dehydrogenase and its isoenzymes as indicators of lung damage or inflammation. *Eur Respir J*. 1996;9(8):1736–42.
39. Van Hoecke L, Job ER, Saelens X, Roose K. Bronchoalveolar Lavage of Murine Lungs to Analyze Inflammatory Cell Infiltration. *J Vis Exp*. *2017*;(123).
40. Chang CC, Tsai ML, Huang HC, Chen CY, Dai SX. Epithelial-mesenchymal transition contributes to SWCNT-induced pulmonary fibrosis. *Nanotoxicology*. 2012;6(6):600–10.
41. Manke A, Luanpitpong S, Dong C, Wang L, He X, Battelli L, et al. Effect of fiber length on carbon nanotube-induced fibrogenesis. *Int J Mol Sci*. 2014;15(5):7444–61.
42. He X, Young SH, Fernback JE, Ma Q. Single-Walled Carbon Nanotubes Induce Fibrogenic Effect by Disturbing Mitochondrial Oxidative Stress and Activating NF-kappaB Signaling. *J Clin Toxicol*. 2012;S5:005.
43. Vietti G, Lison D, van den Brule S. Mechanisms of lung fibrosis induced by carbon nanotubes: towards an Adverse Outcome Pathway (AOP). *Part Fibre Toxicol*. 2016; 13:11.
44. Maeda K, Takahashi K, Takahashi F, Tamura N, Maeda M, Kon S, et al. Distinct roles of osteopontin fragments in the development of the pulmonary involvement in sarcoidosis. *Lung*. 2001;179(5):279–91.
45. Tan TK, Zheng G, Hsu TT, Lee SR, Zhang J, Zhao Y, et al. Matrix metalloproteinase-9 of tubular and macrophage origin contributes to the pathogenesis of renal fibrosis via macrophage recruitment through osteopontin cleavage. *Lab Invest*. 2013;93(4):434–49.
46. Zohar R, Zhu B, Liu P, Sodek J, McCulloch CA. Increased cell death in osteopontin-deficient cardiac fibroblasts occurs by a caspase-3-independent pathway. *Am J Physiol Heart Circ Physiol*. 2004;287(4):H1730–9.
47. Oh K, Seo MW, Kim YW, Lee DS. Osteopontin Potentiates Pulmonary Inflammation and Fibrosis by Modulating IL-17/IFN-gamma-secreting T-cell Ratios in Bleomycin-treated Mice. *Immune Netw*. 2015;15(3):142–9.
48. Raheja LF, Genetos DC, Yellowley CE. Hypoxic osteocytes recruit human MSCs through an OPN/CD44-mediated pathway. *Biochem Biophys Res Commun*. 2008;366(4):1061–6.
49. Kothari AN, Arffa ML, Chang V, Blackwell RH, Syn WK, Zhang J, et al. Osteopontin-A Master Regulator of Epithelial-Mesenchymal Transition. *J Clin Med*. 2016;5(4).
50. Wrana JL, Kubota T, Zhang Q, Overall CM, Aubin JE, Butler WT, et al. Regulation of transformation-sensitive secreted phosphoprotein (SPPI/osteopontin) expression by transforming growth factor-beta. *Comparisons with expression of SPARC (secreted acidic cysteine-rich protein). Biochem J*. 1991;273(Pt 3):523–31.
51. Hullinger TG, Pan Q, Viswanathan HL, Somerman MJ. TGFbeta and BMP-2 activation of the OPN promoter: roles of smad- and hox-binding elements. *Exp Cell Res*. 2001;262(1):69–74.
52. Shi X, Bai S, Li L, Cao X. Hoxa-9 represses transforming growth factor-beta-induced osteopontin gene transcription. *J Biol Chem*. 2001;276(1):850–5.
53. Lenga Y, Koh A, Perera AS, McCulloch CA, Sodek J, Zohar R. Osteopontin expression is required for myofibroblast differentiation. *Circ Res*. 2008;102(3):319–27.
54. Chen YJ, Wei YY, Chen HT, Fong YC, Hsu CJ, Tsai CH, et al. Osteopontin increases migration and MMP-9 upregulation via alphavbeta3 integrin, FAK, ERK, and NF-kappaB-dependent pathway in human chondrosarcoma cells. *J Cell Physiol*. 2009;221(1):98–108.
55. Ding F, Wang J, Zhu G, Zhao H, Wu G, Chen L. Osteopontin stimulates matrix metalloproteinase expression through the nuclear factor-kappaB signaling pathway in rat temporomandibular joint and condylar chondrocytes. *Am J Transl Res*. 2017;9(2):316–29.
56. Driver J, Weber CE, Callaci JJ, Kothari AN, Zapf MA, Roper PM, et al. Alcohol inhibits osteopontin-dependent transforming growth factor-beta1 expression in human mesenchymal stem cells. *J Biol Chem*. 2015;290(16):9959–73.
57. Weber GF, Zawaideh S, Hikita S, Kumar VA, Cantor H, Ashkar S. Phosphorylation-dependent interaction

of osteopontin with its receptors regulates macrophage migration and activation. *J Leukoc Biol*. 2002;72(4):752–61.
58. Rao GV, Tinkle S, Weissman DN, Antonini JM, Kashon ML, Salmen R, et al. Efficacy of a technique for exposing the mouse lung to particles aspirated from the pharynx. *J Toxicol Environ Health A*. 2003;66(15):1441–52.
59. Breen E, Shull S, Burne S, Absher M, Kelley J, Phan S, et al. Bleomycin regulation of transforming growth factor-beta mRNA in rat lung fibroblasts. *Am J Respir Cell Mol Biol*. 1992;6(2):146–52.
60. Takahashi F, Takahashi K, Shimizu K, Cui R, Tada N, Takahashi H, et al. Osteopontin is strongly expressed by alveolar macrophages in the lungs of acute respiratory distress syndrome. *Lung*. 2004;182(3):173–85.
61. Dadrich M, Nicolay NH, Flechsig P, Bickelhaupt S, Hoeltgen L, Roeder F, et al. Combined inhibition of TGFbeta and PDGF signaling attenuates radiation-induced pulmonary fibrosis. *Oncoimmunology*. 2016;5(5):e1123366.
62. Koh A, da Silva AP, Bansal AK, Bansal M, Sun C, Lee H, et al. Role of osteopontin in neutrophil function. *Immunology*. 2007;122(4):466–75.
63. Schneider DJ, Lindsay JC, Zhou Y, Molina JG, Blackburn MR. Adenosine and osteopontin contribute to the development of chronic obstructive pulmonary disease. *FASEB J*. 2010;24(1):70–80.
64. Grotendorst GR, Smale G, Pencev D. Production of transforming growth factor beta by human peripheral blood monocytes and neutrophils. *J Cell Physiol*. 1989;140(2):396–402.
65. Vetrone SA, Montecino-Rodriguez E, Kudryashova E, Kramerova I, Hoffman EP, Liu SD, et al. Osteopontin promotes fibrosis in dystrophic mouse muscle by modulating immune cell subsets and intramuscular TGF-beta. *J Clin Invest*. 2009;119(6):1583–94.
66. Ophascharoensuk V, Giachelli CM, Gordon K, Hughes J, Pichler R, Brown P, et al. Obstructive uropathy in the mouse: role of osteopontin in interstitial fibrosis and apoptosis. *Kidney Int*. 1999;56(2):571–80.
67. Mori R, Shaw TJ, Martin P. Molecular mechanisms linking wound inflammation and fibrosis: knockdown of osteopontin leads to rapid repair and reduced scarring. *J Exp Med*. 2008;205(1):43–51.
68. Singh M, Foster CR, Dalal S, Singh K. Osteopontin: role in extracellular matrix deposition and myocardial remodeling post-MI. *J Mol Cell Cardiol*. 2010;48(3):538–43.
69. Wolak T, Kim H, Ren Y, Kim J, Vaziri ND, Nicholas SB. Osteopontin modulates angiotensin II-induced inflammation, oxidative stress, and fibrosis of the kidney. *Kidney Int*. 2009;76(1):32–43.
70. Yoo KH, Thornhill BA, Forbes MS, Coleman CM, Marcinko ES, Liaw L, et al. Osteopontin regulates renal apoptosis and interstitial fibrosis in neonatal chronic unilateral ureteral obstruction. *Kidney Int*. 2006;70(10):1735–41.
71. Wu M, Schneider DJ, Mayes MD, Assassi S, Arnett FC, Tan FK, et al. Osteopontin in systemic sclerosis and its role in dermal fibrosis. *J Invest Dermatol*. 2012;132(6):1605–14.
72. Coombes JD, Swiderska-Syn M, Dolle L, Reid D, Eksteen B, Claridge L, et al. Osteopontin neutralisation abrogates the liver progenitor cell response and fibrogenesis in mice. *Gut*. 2015;64(7):1120–31.
73. Irita J, Okura T, Jotoku M, Nagao T, Enomoto D, Kurata M, et al. Osteopontin deficiency protects against aldosterone-induced inflammation, oxidative stress, and interstitial fibrosis in the kidney. *Am J Physiol Renal Physiol*. 2011;301(4):F833–44.
74. Inoue M, Moriwaki Y, Arikawa T, Chen YH, Oh YJ, Oliver T, et al. Cutting edge: critical role of intracellular osteopontin in antifungal innate immune responses. *J Immunol*. 2011;186(1):19–23.
75. Pacurari M, Yin XJ, Zhao J, Ding M, Leonard SS, Schwegler-Berry D, et al. Raw single-wall carbon nanotubes induce oxidative stress and activate MAPKs, AP-1, NF-kappaB, and Akt in normal and malignant human mesothelial cells. *Environ Health Perspect*. 2008;116(9):1211–7.
76. Verrecchia F, Vindevoghel L, Lechleider RJ, Uitto J, Roberts AB, Mauviel A. Smad3/AP-1 interactions control transcriptional responses to TGF-beta in a promoter-specific manner. *Oncogene*. 2001;20(26):3332–40.
77. Patarca R, Saavedra RA, Cantor H. Molecular and cellular basis of genetic resistance to bacterial infection: the role of the early T-lymphocyte activation-1/osteopontin gene. *Crit Rev Immunol*. 1993;13(3–4):225–46.
78. Lorenzen JM, Schauerte C, Hubner A, Kolling M, Martino F, Scherf K, et al. Osteopontin is indispensible for AP1-mediated angiotensin II-related miR-21 transcription during cardiac fibrosis. *Eur Heart J*. 2015;36(32):2184–96.
79. Sabo-Attwood T, Ramos-Nino ME, Eugenia-Ariza M, Macpherson MB, Butnor KJ, Vacek PC, et al. Osteopontin modulates inflammation, mucin production, and gene expression signatures after inhalation of asbestos in a murine model of fibrosis. *Am J Pathol*. 2011;178(5):1975–85.
80. Munger JS, Huang X, Kawakatsu H, Griffiths MJ, Dalton SL, Wu J, et al. The integrin alpha v beta 6 binds and activates latent TGF beta 1: a mechanism for regulating pulmonary inflammation and fibrosis. *Cell*. 1999;96(3):319–28.
81. Tatler AL, Jenkins G. TGF-beta activation and lung fibrosis. *Proc Am Thorac Soc*. 2012;9(3):130–6.
82. Standal T, Borset M, Sundan A. Role of osteopontin in adhesion, migration, cell survival and bone remodeling. *Exp Oncol*. 2004;26(3):179–84.
83. He X, Young SH, Schwegler-Berry D, Chisholm WP, Fernback JE, Ma Q. Multiwalled carbon nanotubes induce a fibrogenic response by stimulating reactive oxygen species production, activating NF-kappaB signaling, and promoting fibroblast-to-myofibroblast transformation. *Chem Res Toxicol*. 2011;24(12):2237–48.
84. Wang P, Nie X, Wang Y, Li Y, Ge C, Zhang L, et al. Multiwall carbon nanotubes mediate macrophage activation and

promote pulmonary fibrosis through TGF-beta/Smad signaling pathway. *Small*. 2013;9(22):3799–811.
85. Azad N, Iyer AK, Wang L, Liu Y, Lu Y, Rojanasakul Y. Reactive oxygen species-mediated p38 MAPK regulates carbon nanotube-induced fibrogenic and angiogenic responses. *Nanotoxicology*. 2013;7(2):157–68.
86. Rodan GA Osteopontin overview. *Ann N Y Acad Sci*. 1995;760:1–5.
87. Jang MA, Lee SJ, Baek SE, Park SY, Choi YW, Kim CD. alpha-Iso-Cubebene Inhibits PDGF-Induced Vascular Smooth Muscle Cell Proliferation by Suppressing Osteopontin Expression. *PLoS One*. 2017;12(1):e0170699.
88. Jalvy S, Renault MA, Leen LL, Belloc I, Bonnet J, Gadeau AP, et al. Autocrine expression of osteopontin contributes to PDGF-mediated arterial smooth muscle cell migration. *Cardiovasc Res*. 2007;75(4):738–47.
89. Bostrom K Osteopontin, a missing link in PDGF-induced smooth muscle cell migration. *Cardiovasc Res*. 2007;75(4):634–5.
90. Kusuyama J, Bandow K, Ohnishi T, Hisadome M, Shima K, Semba I, et al. Osteopontin inhibits osteoblast responsiveness through the down-regulation of focal adhesion kinase mediated by the induction of low-molecular weight protein tyrosine phosphatase. *Mol Biol Cell*. 2017;28(10):1326–36.
91. Chen D, Stueckle TA, Luanpitpong S, Rojanasakul Y, Lu Y, Wang L. Gene expression profile of human lung epithelial cells chronically exposed to single-walled carbon nanotubes. *Nanoscale Res Lett*. 2015;10:12.
92. Wang L, Castranova V, Mishra A, Chen B, Mercer RR, Schwegler-Berry D, et al. Dispersion of single-walled carbon nanotubes by a natural lung surfactant for pulmonary in vitro and in vivo toxicity studies. *Part Fibre Toxicol*. 2010;7:31.
93. Taylor AJ, McClure CD, Shipkowski KA, Thompson EA, Hussain S, Garantziotis S, et al. Atomic layer deposition coating of carbon nanotubes with aluminum oxide alters pro-fibrogenic cytokine expression by human mononuclear phagocytes in vitro and reduces lung fibrosis in mice in vivo. *PLoS One*. 2014;9(9):e106870.